frontiers | Frontiers in Physics

TYPE Original Research
PUBLISHED 23 March 2023
DOI 10.3389/fphy.2023.1158814

OPEN ACCESS

EDITED BY
Chengyi Xia,
Tiangong University, China

REVIEWED BY
Qianqian Zheng,
Xuchang University, China
Olumuyiwa James Peter,
University of Medical Sciences, Ondo, Nigeria
Guodong Zhang,
South-Central University for Nationalities, China

*CORRESPONDENCE
Yong Zhou,
zhouyongedu@126.com

SPECIALTY SECTION
This article was submitted to Social Physics, a section of the journal Frontiers in Physics

RECEIVED 04 February 2023
ACCEPTED 09 March 2023
PUBLISHED 23 March 2023

CITATION
Zhou Y, Ding Y and Guo M (2023), Path analysis method in an epidemic model and stability analysis.
Front. Phys. 11:1158814.
doi: 10.3389/fphy.2023.1158814

Path analysis method in an epidemic model and stability analysis

Yong Zhou[1]*, Yiming Ding[1] and Minrui Guo[2]

[1]College of Science, Wuhan University of Science and Technology, Wuhan, China, [2]College of Energy Engineering, Huanghuai University, Zhumadian, China

In this paper, a new method for obtaining the basic reproduction number is proposed, called the path analysis method. Compared with the traditional next-generation method, this method is more convenient and less error-prone. We develop a general model that includes most of the epidemiological characteristics and enumerate all disease transmission paths. The path analysis method is derived by combining the next-generation method and the disease transmission paths. Three typical examples verify the effectiveness and convenience of the method. It is important to note that the path analysis method is only applicable to epidemic models with bilinear incidence rates. The Volterra-type Lyapunov function is given to prove the global stability of the system. The simulations prove the correctness of our conclusions.

KEYWORDS

path analysis method, basic reproduction number, transmission paths, Lyapunov functions, stability

1 Introduction

Research on the epidemic compartment model began with Kermack–McKendrick's SIR [1] system. It took the Black Death as the research object and had only one infected population during the illness period. The advantage of the SIR system is that it only needs to focus on the total number of patients per unit time [2–4]. With the development of medical sciences, it is found that some patients have already been infected before they develop symptoms. Statistics show that most infectious diseases have an asymptomatic infected population, such as COVID-19 [5], SARS [6], and Ebola [7]. Therefore, scholars proposed the SIR [8–11] model with two infected populations: asymptomatic and symptomatic populations. The asymptomatic population is transformed into a symptomatic population by a certain percentage after a latent period.

In recent years, researchers have developed more complex high-dimensional models based on the transmission characteristics. In [12], the $\mathbf{S}E_1E_2I_1I_2HR$ model for COVID-19 in Wuhan was established. Infected individuals were divided into four populations, of which $E_2, I_1 \mathbf{and} I_2$ were infectious. In [13], the SEQAIJR model consisting of quarantined and isolated populations was developed. The authors divided patients into five populations, four of which were infectious, except for those in the incubation period. In [14], the SCEAIHR model divided people into seven populations, but only three were infectious. Actually, most models divide infected people into multiple populations, but not all are infectious [15–17]. This phenomenon will be fully reflected in the basic reproduction number.

The basic reproduction number [18–23] is one of the most important indicators of the infectious disease compartment model. Its basic form is $R_0 = K\beta/\mu$ [24], where $\boldsymbol{K}$ is the total population, $\boldsymbol{\beta}$ is the infection rate, and $\boldsymbol{\mu}$ is the elimination rate. When there are multiple compartments, it becomes $R_0 = R_{0(1)} + R_{0(2)} + \cdots + R_{0(n)}$ [25, 26]. Usually, it can be solved

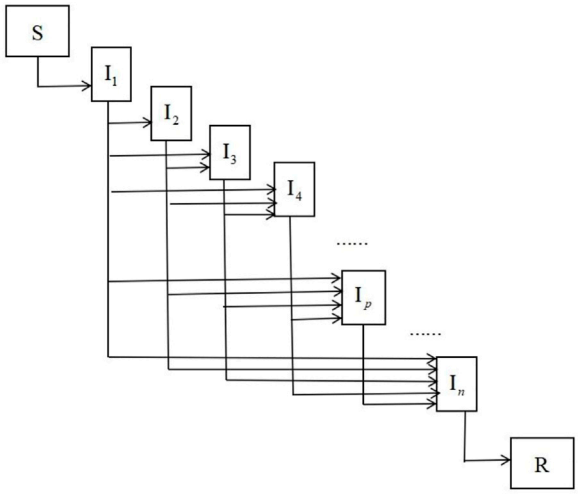

FIGURE 1
Disease transmission paths.

by the next-generation method. The value of $\boldsymbol{n}$ depends on the infected populations that are infectious, since a proportion of infected individuals are isolated.

The study of stability is one of the most important subjects in the infectious disease model. Many studies [27–35] give the methods for proving the local and global stabilities of the singularities. Lyapunov's second method and Lasalle's invariance principle are the most common methods for proving global stability. However, they are not easy to operate because there is no general way to construct a suitable Lyapunov function. In the Lyapunov function toolbox, linear-, quadratic-, and Volterra-type functions are three frequently used functions applied to biological systems. These functions are as follows:

$$V_1(x_1, x_2, \cdots, x_n) = \sum_{i=1}^{n} m_i x_i,$$

$$V_2(x_1, x_2, \cdots, x_n) = \sum_{i=1}^{n} \frac{m_i}{2}(x_i - x_i^*)^2,$$

$$V_3(x_1, x_2, \cdots, x_n) = \sum_{i=1}^{n} m_i\left(x_i - x_i^* - x_i^* \ln \frac{x_i}{x_i^*}\right),$$

where $m_i > 0, i = 1, 2, \cdots, n$. In most cases, it requires linear- and Volterra-type functions to prove the global stabilities of disease-free and endemic equilibrium points, respectively. In [36], a linear-type Lyapunov function to prove the global stability of the disease-free equilibrium was defined. In [37], Ottaviano et al. constructed a suitable Lyapunov function based on the Volterra-type function for the endemic equilibrium point.

In summary, most researchers introduce their models, then calculate the basic reproduction number, and prove the stability of the equilibrium point. These processes are similar but require tedious calculations. Is it possible to obtain a basic reproduction number with universal applicability by building a general model containing the main features? This paper develops a model with n infected populations that can only be transferred from top to bottom. We list all transmission paths and find some important conclusions. The number of the transmission paths for the final infected population is the sum of the combinatorial numbers. The number for all infected populations is twice the sum of the combination numbers. The basic reproduction number of the system is derived by the next-generation method. By decomposing the basic reproduction number formula, we find not all infected populations are infectious, such as those who are isolated and treated. A path analysis method is shown by combining the basic reproduction number formula with the disease transmission paths. This method greatly simplifies the calculation and it is successfully applied in three typical examples. The paper also gives the conditions for the existence of disease-free and endemic equilibrium points. Their global stabilities are proved by two Lyapunov functions with linear- and Volterra-type tools. Simulations verify the conclusions.

TABLE 1 Simulation parameter values for chapter 5.

I_n	Transmission path	Number
I_1	$S \to I_1$	1
I_2	$I_1 \to I_2$	1
I_3	$I_1 \to I_3, I_1 \to I_2 \to I_3$	2
I_4	$I_1 \to I_4, I_1 \to I_2 \to I_4, I_1 \to I_3 \to I_4,$ $I_1 \to I_2 \to I_3 \to I_4$	4
I_5	$I_1 \to I_5, I_1 \to I_2 \to I_5, I_1 \to I_3 \to I_5,$ $I_1 \to I_4 \to I_5, I_1 \to I_2 \to I_3 \to I_5,$ $I_1 \to I_2 \to I_4 \to I_5, I_1 \to I_3 \to I_4 \to I_5,$ $I_1 \to I_2 \to I_3 \to I_4 \to I_5$	8
…	…	…
I_n	$I_1 \to I_n, \cdots$	2^{n-2}
Total		2^{n-1}

2 Model and method

Individuals are divided into three categories, susceptible (S), infected (I), and recovered (R) populations. Infected populations are divided into n populations, which can be denoted as $I_1, I_2, \cdots, I_n$. I_1 is the asymptomatic population, and $I_2, I_3, \cdots, I_n$ are symptomatic populations. All symptomatic infected individuals go through an asymptomatic period. I_i comes from $I_1, I_2, \cdots, I_{i-1}$ and will be transferred to $I_{i+1}, I_{i+2}, \cdots, I_n$ with $1 < i < n$. The compartment model can be represented by Figure 1 and system 1. The incidence rate is $\sum_{i=1}^{n} \beta_i S I_i$. The input rate and natural mortality are Λ and μ. μ_i is the mortality of I_i. r_q^p represents the conversion rate from I_p to I_q. The transmission paths are shown in Table 1. It can be concluded that I_n comes from 2^{n-2} paths: $2^{n-2} = C_{n-2}^0 + C_{n-2}^1 + C_{n-2}^2 + \cdots + C_{n-2}^{n-2}$. The number of the paths for I_n is equal to the sum of all combinatorial numbers. The sum of the total transmission paths of $I_1, I_2, I_3, \cdots, I_n$ is 2^{n-1}. The total population is $N = S + \sum_{i=1}^{n} I_i + R$. By deriving the equation, we obtain the following equation:

$$\frac{dN}{dt} = \frac{d\left(S + \sum_{i=1}^{n} I_i + R\right)}{dt} = \Lambda - \sum_{i=1}^{n} \mu_i I_i - \mu N(t) \le \Lambda - \mu N(t),$$

$$\begin{cases} \dfrac{dS}{dt} = \Lambda - \sum_{p=1}^{n} \beta_p S I_p - \mu S, \\ \dfrac{dI_1}{dt} = \sum_{p=1}^{n} \beta_p S I_p - \left(\mu_1 + \sum_{p=2}^{n} r_p^1\right) I_1, \\ \dfrac{dI_2}{dt} = r_2^1 I_1 - \left(\mu_2 + \sum_{p=3}^{n} r_p^2\right) I_2, \\ \cdots \\ \dfrac{dI_p}{dt} = \sum_{p=1}^{q-1} r_q^p I_p - \left(\mu_q + \sum_{p=q+1}^{n} r_p^q\right) I_q, \ (q = 4, 5, \cdots, n-1), \\ \cdots \\ \dfrac{dI_n}{dt} = \sum_{p=1}^{n-1} r_n^p I_p - (\mu_n + r_{n+1}^n) I_n, \\ \dfrac{dR}{dt} = r_{n+1}^n I_n - \mu R, \end{cases} \tag{1}$$

$$N(t) \le \frac{\Lambda}{\mu} - \frac{C_0}{\mu} e^{-\mu t}, C_0 > 0.$$

Here, the next-generation method [38] is used to calculate the basic reproduction number. We rewrite system 1 as $(I_1, I_2, I_3, \cdots, I_n, S, R)$. It can be expressed as follows:

$$r_i(x) = \begin{bmatrix} \sum_{p=1}^{n} \beta_p S I_p \\ 0 \\ \vdots \\ 0 \end{bmatrix}, \ h_i(x) = \begin{bmatrix} \left(\mu_1 + \sum_{p=2}^{n} r_p^1\right) I_1 \\ -r_2^1 I_1 + \left(\mu_2 + \sum_{p=3}^{n} r_p^1\right) I_2 \\ \vdots \\ -r_{n+1}^n I_n + \mu R \end{bmatrix}.$$

F and V are the Jacobian matrices of $r_i(x)$ and $h_i(x)$. Then, we obtain

$$F = \frac{\partial r_i}{\partial x_j}(x_0) = \begin{bmatrix} \beta_1 \frac{\Lambda}{\mu} & \beta_2 \frac{\Lambda}{\mu} & \beta_3 \frac{\Lambda}{\mu} & \cdots & \beta_n \frac{\Lambda}{\mu} & 0 & 0 \\ 0 & 0 & 0 & \cdots & 0 & 0 & 0 \\ \vdots & \vdots & \vdots & \ddots & \vdots & \vdots & \vdots \\ 0 & 0 & 0 & \cdots & 0 & 0 & 0 \end{bmatrix},$$

$$V = \frac{\partial h_i}{\partial x_j}(x_0)$$

$$= \begin{bmatrix} \mu_1 + \sum_{p=2}^{n} r_p^1 & 0 & 0 & \cdots & 0 & 0 & 0 & 0 \\ -r_2^1 & \mu_2 + \sum_{p=3}^{n} r_p^2 & 0 & \cdots & 0 & 0 & 0 & 0 \\ -r_3^1 & -r_3^2 & \mu_3 + \sum_{p=4}^{n} r_p^3 & \cdots & 0 & 0 & 0 & 0 \\ \vdots & \vdots & \vdots & \ddots & \vdots & \vdots & \vdots & \vdots \\ -r_n^1 & -r_n^2 & -r_n^3 & \cdots & -r_n^{n-1} & \mu_n + r_{n+1}^n & 0 & 0 \\ \beta_1 \frac{\Lambda}{\mu} & \beta_2 \frac{\Lambda}{\mu} & \beta_3 \frac{\Lambda}{\mu} & \cdots & \beta_{n-1} \frac{\Lambda}{\mu} & \beta_n \frac{\Lambda}{\mu} & \mu & 0 \\ 0 & 0 & 0 & \cdots & 0 & r_n^{n-1} & 0 & \mu \end{bmatrix},$$

where $1 \le i, j \le n$. The basic reproduction number R_0 is the spectral radius of FV^{-1}. The elements of F are all zero except these at the first row. So, we only need to consider the first column of V^{-1}. It is given by

$$V^{-1} = \frac{\partial h_i}{\partial x_j}(x_0) = \begin{bmatrix} \frac{1}{A_1} & \cdots & \cdots \\ \frac{r_2^1}{A_1 A_2} & \cdots & \cdots \\ \frac{r_2^1 r_3^2 + r_3^1 A_2}{A_1 A_2 A_3} & \cdots & \cdots \\ \vdots & \vdots & \vdots \\ \frac{\sum_{p=0}^{n-2} B_{n-2}^p}{\prod_{i=1}^{n} A_i} & \cdots & \cdots \\ 0 & \vdots & \vdots \\ 0 & \vdots & \vdots \end{bmatrix}, A_i = \mu_i + \sum_{p=i+1}^{n} r_p^1, i = 1, 2, \cdots, n,$$

where

$$B_{n-2}^0 = r_n^1 \prod_{i=2}^{n} A_i,$$

$$B_{n-2}^1 = \sum_{p=2}^{n-1} r_p^1 r_n^p \prod_{i=2}^{p-1} A_i \prod_{i=p+1}^{n-1} A_i,$$

$$B_{n-2}^2 = \sum_{p_1=2, p_2=3, p_2 > p_1}^{n-1} r_{p_1}^1 r_{p_2}^{p_1} r_n^{p_2} \prod_{i=2}^{p_1-1} A_i \prod_{i=p_1+1}^{p_2-1} A_i \prod_{i=p_2+1}^{n-1} A_i,$$

$$B_{n-2}^3 = \sum_{p_1=2, p_2=3, p_3=4, p_3 > p_2 > p_1}^{n-1} r_{p_1}^1 r_{p_2}^{p_1} r_{p_3}^{p_2} r_n^{p_3} \prod_{i=2}^{p_1-1} A_i \prod_{i=p_1+1}^{p_2-1} A_i \prod_{i=p_2+1}^{p_3-1} A_i \prod_{i=p_3+1}^{n-1} A_i,$$

$$\cdots\cdots, B_{n-2}^{n-2} = \prod_{i=1}^{i=n-1} r_{i+1}^i.$$

Hence,

$$FV^{-1} = \begin{bmatrix} R_{0(I_1)} + R_{0(I_2)} + R_{0(I_3)} + R_{0(I_4)} + \cdots + R_{0(I_n)} & \cdots & \cdots \\ 0 & 0 & 0 \\ \vdots & \vdots & \vdots \\ 0 & 0 & 0 \\ 0 & 0 & 0 \end{bmatrix},$$

$$R_0 = \rho\left(FV^{-1}\right) = R_{0(I_1)} + R_{0(I_2)} + R_{0(I_3)} + R_{0(I_4)} + \cdots + R_{0(I_n)},$$

where

$$R_{0(I_1)} = \beta_1 \frac{\Lambda}{\mu} \frac{1}{A_1},$$

$$R_{0(I_2)} = \beta_2 \frac{\Lambda}{\mu} \frac{r_2^1}{A_1 A_2} = \beta_2 \frac{\Lambda}{\mu} \frac{r_2^1}{A_1} \frac{1}{A_2},$$

$$R_{0(I_3)} = \beta_3 \frac{\Lambda}{\mu} \frac{r_3^1 A_2 + r_2^1 r_3^2}{A_1 A_2 A_3} = \beta_3 \frac{\Lambda}{\mu} \left(\frac{r_3^1}{A_1} + \frac{r_2^1 r_3^2}{A_1 A_2}\right) \frac{1}{A_3},$$

$$R_{0(I_4)} = \beta_4 \frac{\Lambda}{\mu} \frac{r_4^1 A_2 A_3 + r_2^1 r_4^2 A_3 + r_3^1 r_4^3 A_2 + r_2^1 r_3^2 r_4^3}{A_1 A_2 A_3 A_4}$$

$$= \beta_4 \frac{\Lambda}{\mu} \left(\frac{r_4^1}{A_1} + \frac{r_2^1 r_4^2}{A_1 A_2} + \frac{r_3^1 r_4^3}{A_1 A_3} + \frac{r_2^1 r_3^2 r_4^3}{A_1 A_2 A_3}\right) \frac{1}{A_4}, \cdots\cdots,$$

$$R_{0(I_n)} = \beta_n \frac{\Lambda}{\mu} \frac{C_{n-2}^0 + C_{n-2}^1 + \cdots + C_{n-2}^{n-2}}{\prod_{i=1}^{n} A_i}$$

$$= \beta_n \frac{\Lambda}{\mu} \left(\frac{r_n^1}{A_1} + \frac{r_2^1 r_n^2}{A_1 A_2} + \cdots + \frac{r_2^1 r_3^2 r_n^3}{A_1 A_2 A_3} + \cdots + \frac{\prod_{i=1}^{i=n-1} r_{i+1}^i}{\prod_{i=1}^{n-1} A_i}\right) \frac{1}{A_n}.$$

Here, the basic reproduction number consists of $R_{0(I_i)}$ that is contributed by I_i. A_i represents the elimination rate of infected population I_i, and $1/A_i$ can be seen as the illness period. It is found that $R_{0(I_i)}$ is equal to the product of infection rate, population size, and illness period. I_1 comes from 1 path $S \to I_1$. Its population size is Λ/μ. The infection and elimination rates are β_1 and $1/A_1$. I_1 contributes $\beta_1\Lambda/(\mu A_1)$. I_2 comes from 1 path $I_1 \to I_2$. Its population size is $\Lambda r_2^1/(\mu A_1)$. The infection and elimination rates are β_2 and $1/A_2$. I_2 contributes $\beta_2\Lambda r_2^1/(\mu A_1 A_2)$. I_3 comes from 2 paths $I_1 \to I_3$, $I_1 \to I_2 \to I_3$. Its population size is from I_1 and I_2, which can be shown as $\Lambda r_3^1/(\mu A_1)$ and $\Lambda r_2^1 r_3^2/(\mu A_1 A_2)$. The infection and elimination rates are β_3 and $1/A_3$. So, I_3 contributes $\beta_3\Lambda r_3^1/(\mu A_1 A_3) + \beta_3\Lambda r_2^1 r_3^2/(\mu A_1 A_2 A_3)$. The contribution of I_n can be obtained by analogy. Thus, we can get the basic reproduction number with very little calculations. We define this process as a path analysis method that can be applied for the bilinear compartment models. The key is to find out all transmission paths and different population sizes.

3 Application examples

For high-dimensional epidemic model, it is cumbersome and error-prone to derive the basic reproduction number using the next-generation method. In this section, we use the path analysis method of Section 2 to directly give the basic reproduction numbers for three bilinear compartment models without any calculation.

In [37], system (2) has two populations with infection capability, which are called asymptomatic $A(t)$ and infected $I(t)$ populations. $A(t)$ comes from the path $S \to A$, and $I(t)$ comes from the path $A \to I$. According to the path analysis method, the basic reproduction number can be expressed as $R_0 = R_{0_A} + R_{0_I}$. The total population is $(\mu+\gamma)/(\mu+\nu+\gamma)$ through the first equation of the system. The population sizes of $A(t)$ and $I(t)$ are $(\mu+\gamma)/(\mu+\nu+\gamma)$ and $\alpha(\mu+\gamma)/[(\mu+\nu+\gamma)\ (\alpha+\delta_A+\mu)]$. The infection rates of $A(t)$ and $I(t)$ are β_A and β_I. The elimination rates are $1/(\alpha+\delta_A+\mu)$ and $1/(\delta_I+\mu)$. $A(t)$ and $I(t)$ contribute

$$R_{0_A} = \beta_A \frac{\mu+\gamma}{\mu+\nu+\gamma}\frac{1}{\alpha+\delta_A+\mu},\ R_{0_I} = \beta_I \frac{\mu+\gamma}{\mu+\nu+\gamma}\frac{1}{\delta_I+\mu}.$$

Therefore, the basic reproduction number is as follows:

$$R_0 = \beta_A \frac{\mu+\gamma}{\mu+\nu+\gamma}\frac{1}{\alpha+\delta_A+\mu} + \beta_I \frac{\mu+\gamma}{\mu+\nu+\gamma}\frac{1}{\delta_I+\mu},$$

$$\begin{cases} \dfrac{dS(t)}{dt} = \mu - (\beta_A A(t) + \beta_I I(t))S(t) - (\mu+\nu)S(t) + \gamma R(t), \\ \dfrac{dA(t)}{dt} = (\beta_A A(t) + \beta_I I(t))S(t) - (\alpha+\delta_A+\mu)A(t), \\ \dfrac{dI(t)}{dt} = \alpha A(t) - (\delta_I+\mu)I(t), \\ \dfrac{dR(t)}{dt} = \delta_A A(t) + \delta_I I(t) + \nu S(t) - (\gamma+\mu)R(t). \end{cases} \tag{2}$$

System (3) with nine dimensions has been developed in [25] to depict the transmission of COVID-19. The first equation reveals that I_{ss}, I_{ms}, and I_a are infectious. I_{ss}, I_{ms}, and I_a come from the paths $S \to E \to I_{ss}$, $S \to E \to I_{ms}$, and $S \to E \to I_a$, respectively. So, the basic reproduction number can be

$$\begin{cases} \dfrac{dS(t)}{dt} = -\beta\dfrac{S(t)}{N}(I_{ss}(t) + I_{ms}(t) + I_a(t)), \\ \dfrac{dE(t)}{dt} = \beta\dfrac{S(t)}{N}(I_{ss}(t) + I_{ms}(t) + I_a(t)) - kE(t), \\ \dfrac{dI_{ss}(t)}{dt} = kp_1E(t) - hI_{ss}(t), \\ \dfrac{dI_{ms}(t)}{dt} = kp_2E(t) - \gamma_3 I_{ms}(t), \\ \dfrac{dI_a(t)}{dt} = k(1-p_1-p_2)E(t) - \gamma_3 I_a(t), \\ \dfrac{dH(t)}{dt} = hq_1 I_{ss}(t) - H(t), \\ \dfrac{dI_{cu}(t)}{dt} = h(1-q_1)I_{ss}(t) - I_{cu}, \\ \dfrac{dR(t)}{dt} = \gamma_3 I_{ms}(t) + \gamma_3 I_a(t) + (1-\delta_1)H(t) + (1-\gamma_1)I_{cu}(t), \\ \dfrac{dD(t)}{dt} = \delta_1 H(t) + \gamma_1 I_{cu}(t), \end{cases} \tag{3}$$

shown as $R_0 = R_{0_{I_{ss}}} + R_{0_{I_{ms}}} + R_{0_{I_a}}$. The infection rates of the three populations are β. The elimination rates of I_{ss}, I_{ms}, and I_a are $1/h$, $1/\gamma_3$, and $1/\gamma_3$. The population sizes of I_{ss}, I_{ms}, and I_a are p_1, p_2, and $1-p_1-p_2$. I_{ss}, I_{ms}, and I_a contribute

$$R_{0_{I_{ss}}} = \beta\frac{p_1}{h},\ R_{0_{I_{ms}}} = \beta\frac{p_2}{\gamma_3},\ R_{0_a} = \beta\frac{1-p_1-p_2}{\gamma_3}.$$

The basic reproduction number is as follows:

$$R_0 = \beta\frac{p_1}{h} + \beta\frac{p_2}{\gamma_3} + \beta\frac{1-p_1-p_2}{\gamma_3},$$

$$\begin{cases} \dfrac{dS}{dt} = \Pi - \dfrac{S(\beta I + r_Q\beta Q + r_A\beta A) + r_J\beta J}{N} - \mu S, \\ \dfrac{dE}{dt} = \dfrac{S(\beta I + r_Q\beta Q + r_A\beta A) + r_J\beta J}{N} - (\gamma_1 + k_1 + \mu)E, \\ \dfrac{dQ}{dt} = \gamma_1 E - (k_2 + \sigma_1 + \mu)Q, \dfrac{dA}{dt} = pk_1E - (\sigma_2+\mu)A, \\ \dfrac{dI}{dt} = (1-p)k_1E - (\gamma_2 + \sigma_3 + \mu)I, \\ \dfrac{dJ}{dt} = k_2Q + \gamma_2 I - (\delta + \sigma_4 + \mu)J, \\ \dfrac{dR}{dt} = \sigma_1 Q + \sigma_2 A + \sigma_3 I + \sigma_4 J - \mu R. \end{cases} \tag{4}$$

In [13], an epidemic model (4) incorporating quarantine was built to predict the COVID-19 trend in the United Kingdom. The first equation shows that the quarantine $Q(t)$, asymptomatic $A(t)$, symptomatic $I(t)$, and isolated $J(t)$ populations are infectious in this system. $Q(t)$, $A(t)$, and $I(t)$ come from the paths $S \to E \to Q$, $S \to E \to A$, and $S \to E \to I$. $J(t)$ is from two paths $S \to E \to Q \to J$ and $S \to E \to I \to J$. The basic reproduction number can be denoted as $R_0 = R_{0_Q} + R_{0_A} + R_{0_I} + R_{0_{J_1}} + R_{0_{J_2}}$. The population sizes of $Q(t)$, $A(t)$, and $I(t)$ are 1. The population size of $J(t)$ can be divided into

two parts. One part from $Q(t)$ is $k_2/(k_2+\sigma_1+\mu)$. The other part from $I(t)$ is $\gamma_2/(\gamma_2+\sigma_3+\mu)$. The infection rates of $Q(t)$, $A(t)$, $I(t)$, and $J(t)$ are $r_Q\beta$, $r_A\beta$, β, and $r_J\beta$. The elimination rates are $1/(k_2+\sigma_1+\mu)$, $1/(\sigma_2+\mu)$, $1/(\gamma_2+\sigma_3+\mu)$ and $1/(\delta+\sigma_4+\mu)$. $Q(t)$, $A(t)$, $I(t)$, and $J(t)$ contribute

$$R_{0_Q}=r_Q\beta\frac{1}{k_2+\sigma_1+\mu},\ R_{0_A}=r_A\beta\frac{1}{\sigma_2+\mu},\ R_{0_I}=\beta\frac{1}{\gamma_2+\sigma_3+\mu},$$
$$R_{0_J}=r_J\beta\frac{k_2}{k_2+\sigma_1+\mu}\frac{1}{\delta+\sigma_4+\mu}+r_J\beta\frac{\gamma_2}{\gamma_2+\sigma_3+\mu}\frac{1}{\delta+\sigma_4+\mu}.$$

The basic reproduction number is

$$R_0=r_Q\beta\frac{1}{k_2+\sigma_1+\mu}+r_A\beta\frac{1}{\sigma_2+\mu}+\beta\frac{1}{\gamma_2+\sigma_3+\mu}$$
$$+r_J\beta\frac{k_2}{k_2+\sigma_1+\mu}\frac{1}{\delta+\sigma_4+\mu}+r_J\beta\frac{\gamma_2}{\gamma_2+\sigma_3+\mu}\frac{1}{\delta+\sigma_4+\mu}.$$

4 Global stability analysis

4.1 Global stability analysis of the disease-free equilibrium point

Theorem 4.1: The disease-free equilibrium point of system (1) is $(\Lambda/\mu,0,0,\cdots,0)$. It is globally stable if $R_0<1$.

Proof. Let $I_i=R=0, i=1,2,\cdots,n$. Then, we get $(\Lambda/\mu,0,0,\cdots,0)$ as the disease-free equilibrium point. We define a linear function as follows:

$$V=\sum_{i=1}^{n}m_iI_i,$$

where $m_q=\frac{\sum_{p=0}^{n-q}\beta_{q+p}\frac{\Lambda}{\mu}\prod_{i=q+p+1}^{n}A_i\prod_{i=q}^{q+p-1}r_{i+1}^{i}}{\prod_{i=q}^{n}A_i}r_q^1$, $i=1,2,\cdots,q,\cdots,n$. Calculating the time derivative of V along the solutions of system (1), we have

$$\begin{aligned}\frac{dV}{dt}&=m_1\left[\sum_{p=1}^{n}\alpha_pSI_p-\left(\mu_1+\sum_{p=2}^{n}r_p^1\right)I_1\right]\\&+m_2\left[r_2^1I_1-\left(\mu_2+\sum_{p=3}^{n}r_p^1\right)I_2\right]+\cdots+m_n\left[\sum_{p=1}^{n-1}r_n^pI_p-(\mu_n+r_{n+1}^n)I_n\right],\\&\le\left(m_1\beta_1\frac{\Lambda}{\mu}-m_1A_1+m_2r_2^1+m_3r_3^1+\cdots+m_nr_n^1\right)I_1,\\&=\left(\frac{\beta_1\frac{\Lambda}{\mu}}{A_1}+\frac{m_2r_2^1}{A_1}+\frac{m_3r_3^1}{A_1}+\cdots+\frac{m_nr_n^1}{A_1}-1\right)A_1I_1,\\&=\left(\frac{\beta_1\frac{\Lambda}{\mu}}{A_1}+\frac{\sum_{i=2}^{n}m_{2(\beta_i)}r_2^1}{A_1}+\frac{\sum_{i=3}^{n}m_{3(\beta_i)}r_3^1}{A_1}+\cdots+\frac{\sum_{i=n}^{n}m_{n(\beta_i)}r_n^1}{A_1}-1\right)A_1I_1,\\&=(R_0-1)A_1I_1.\end{aligned}$$

When $R_0<1$, $\frac{dV}{dt}<0$. According to Lyapunov's second method [39–43], the disease-free equilibrium point is globally stable.

4.2 Global stability analysis of the endemic equilibrium point

Theorem 4.2: When $R_0>1$, system (1) has an endemic equilibrium point, and it is globally stable.

Proof. According to the equilibrium solution of system (1), we can arrive at

$$I_1=\frac{\Lambda(\beta_1+\beta_2B_2+\beta_3B_3+\cdots+\beta_nB_n)-\mu A_1}{A_1(\beta_1+\beta_2B_2+\beta_3B_3+\cdots+\beta_nB_n)}>0,$$
$$\frac{\Lambda(\beta_1+\beta_2B_2+\beta_3B_3+\cdots+\beta_nB_n)}{\mu A_1}-1>0,$$
$$R_0-1>0.$$

Therefore, when $R_0>1$, system (1) has an endemic equilibrium point. The endemic equilibrium point can be represented as $(S^*,I_1^*,I_2^*,\cdots,I_n^*,R^*)$. We define a Volterra-type Lyapunov function

$$L(S,I_1,I_2,\cdots,I_n)=m_0\left(S-S^*-S^*\ln\frac{S}{S^*}\right)+\sum_{p=1}^{n}m_p\left(I_p-I_p^*-I_p^*\ln\frac{I_p}{I_p^*}\right).$$

We denote

$$m_1=m_0,m_k=m_0\frac{\beta_kS^*I_k^*}{r_k^1I_1^*},k=2,3,4,\cdots,n.$$

Differentiating L along system (1), we have

$$\begin{aligned}\frac{dL}{dt}\le&m_0\sum_{p=1}^{n}\beta_pS^*I_p^*\left(1-\frac{SI_p}{S^*I_p^*}\right)\left(1-\frac{S^*}{S}\right)+m_0\mu S^*\left(1-\frac{S}{S^*}\right)\left(1-\frac{S^*}{S}\right)\\&+m_1\sum_{p=1}^{n}\left(\beta_p\frac{SI_p}{S^*I_p^*}-\frac{I_1}{I_1^*}\right)\left(1-\frac{I_1^*}{I_1}\right)+\cdots+m_q\sum_{p=1}^{q-1}r_q^pI_p^*\left(\frac{I_p}{I_p^*}-\frac{I_q}{I_q^*}\right)\\&\times\left(1-\frac{I_q^*}{I_q}\right)+m_q\sum_{p=q+1}^{n}t_pI_p^*\left(\frac{I_p}{I_p^*}-\frac{I_q}{I_q^*}\right)\left(1-\frac{I_q^*}{I_q}\right)+\cdots\\&+m_n\sum_{p=1}^{n-1}r_n^pI_p^*\left(\frac{I_p}{I_p^*}-\frac{I_n}{I_n^*}\right)\left(1-\frac{I_n^*}{I_n}\right).\end{aligned}$$

By calculation, we can get

$$\begin{aligned}\frac{dL}{dt}\le&m_0\sum_{p=1}^{n}\beta_nS^*I_n^*\left(1-\frac{S^*}{S}+\frac{I_n}{I_n^*}-\frac{SI_n}{S^*I_n^*}\right)+m_0\mu S^*\left(2-\frac{S}{S^*}-\frac{S^*}{S}\right)\\&+m_1\beta_1S^*I_1^*\left(1-\frac{S}{S^*}-\frac{I_1}{I_1^*}+\frac{SI_1}{S^*I_1^*}\right)+\sum_{p=2}^{n}m_1\beta_pS^*I_p^*\left(1-\frac{SI_1^*I_p}{S^*I_1I_p^*}-\frac{I_1}{I_1^*}+\frac{SI_p}{S^*I_p^*}\right)\\&+\cdots\\&+m_q\sum_{p=1}^{q-1}r_q^pI_p^*\left(1+\frac{I_p}{I_p^*}-\frac{I_q}{I_q^*}-\frac{I_pI_q^*}{I_p^*I_q}\right)+m_q\sum_{p=q+1}^{n}t_pI_p^*\left(1+\frac{I_p}{I_p^*}-\frac{I_q}{I_q^*}-\frac{I_pI_q^*}{I_p^*I_q}\right)\\&+\cdots\\&+m_n\sum_{p=1}^{n-1}r_n^pI_p^*\left(1+\frac{I_p}{I_p^*}-\frac{I_n}{I_n^*}-\frac{I_pI_n^*}{I_p^*I_n}\right).\end{aligned}$$

Finally, we get

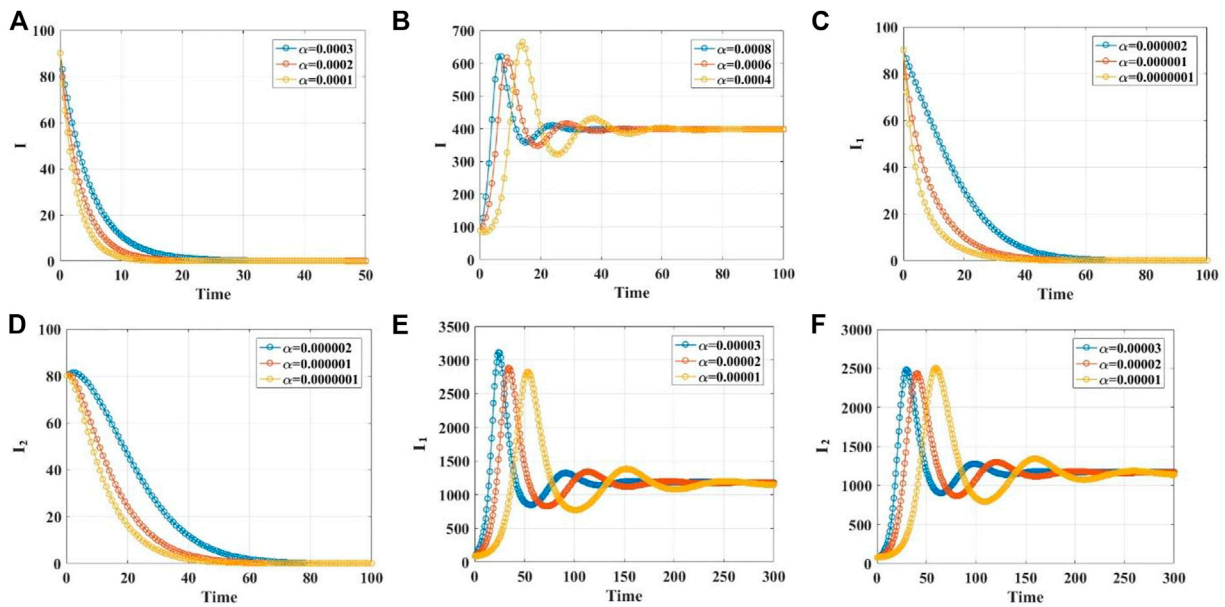

FIGURE 2
(A, B) The time series diagrams for $n = 1$. **(C–F)** The time series diagrams for $n = 2$.

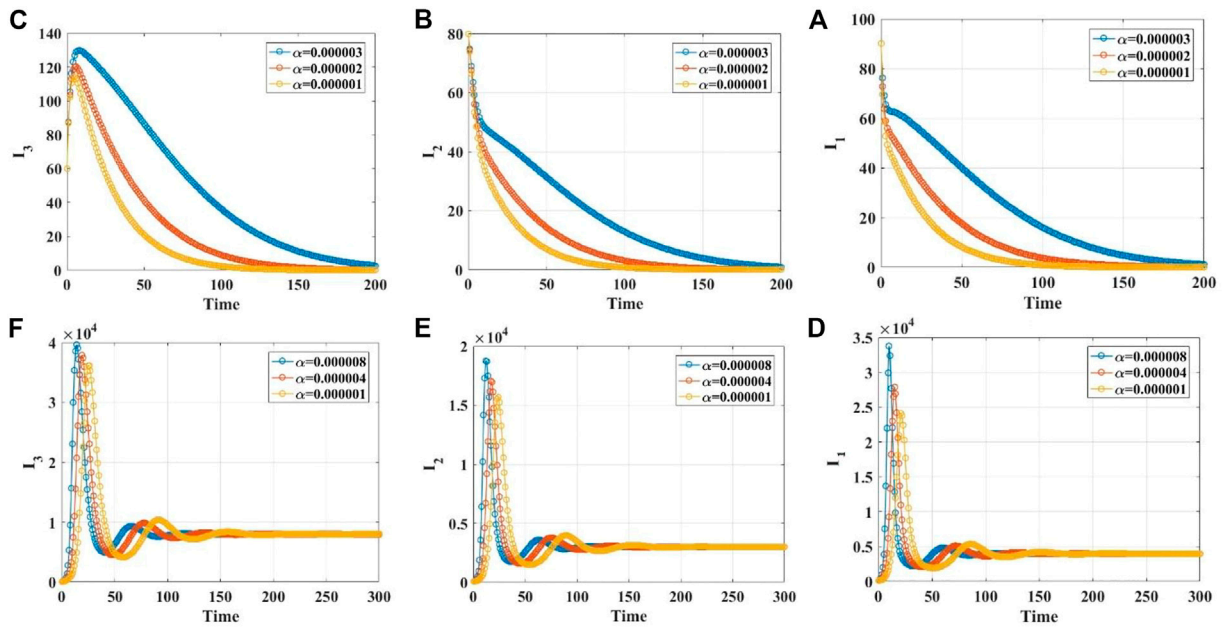

FIGURE 3
The time series diagrams for $n = 3$.

$$\frac{dL}{dt} \le m_0 S^* I_1^* (\mu + \beta_1)\left(2 - \frac{S^*}{S} - \frac{S}{S^*}\right) + m_0 S^* \sum_{p=2}^{n} \beta_p I_p^* \left(3 - \frac{S^*}{S} - \frac{S I_1^* I_p}{S^* I_1 I_p^*} - \frac{I_1 I_p^*}{I_1^* I_p}\right) < 0.$$

According to Lyapunov's second method, the endemic equilibrium point is globally stable.

5 Model simulation

We demonstrate the stabilities of the disease-free and endemic equilibrium points with 1, 2, 3, and 4 infected populations through simulations. Supplementary Material S1 gives the values of the parameters in different cases. When the infection rate α of I_1 is taken as 0.0001, 0.0002, and 0.0003,

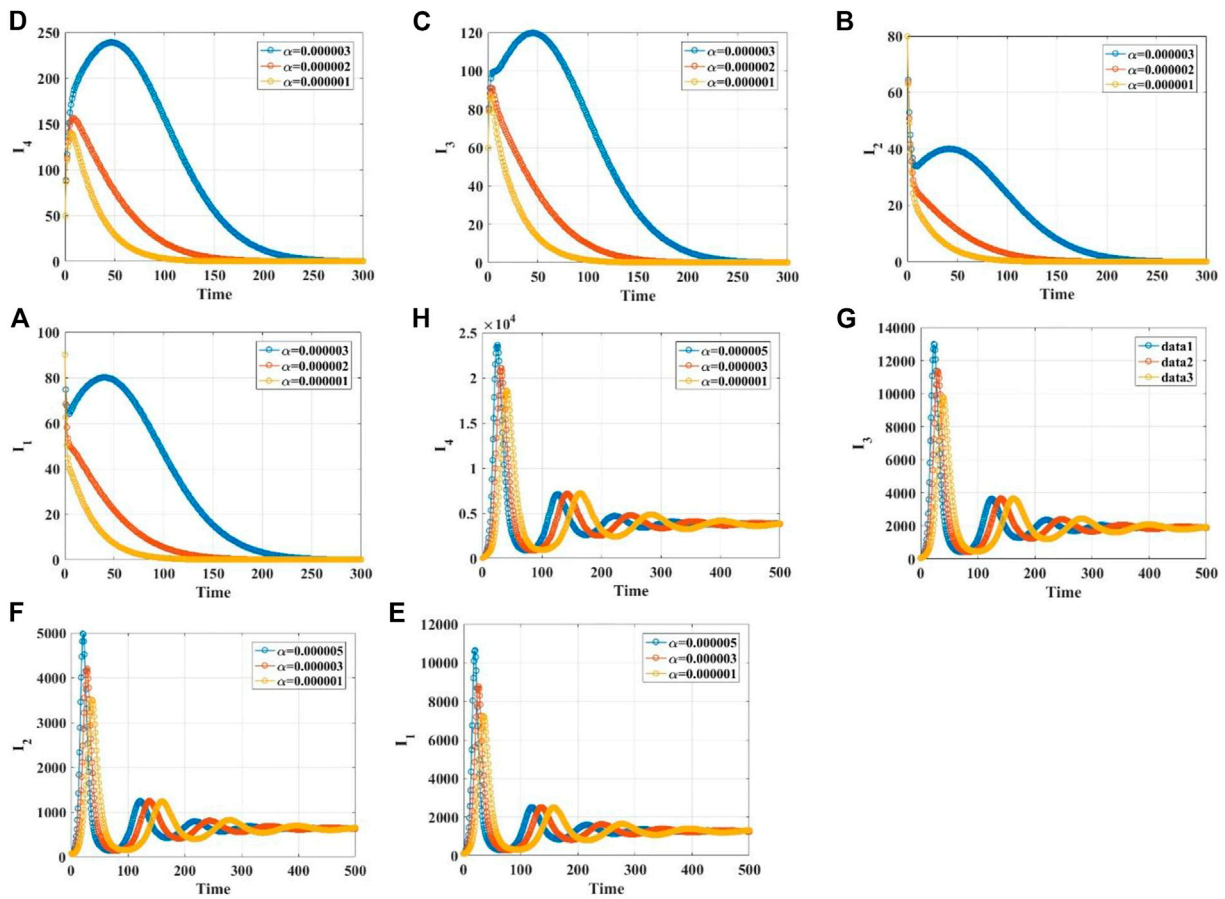

FIGURE 4
The time series diagrams for $n = 4$.

Figure 2A demonstrates the global stability of the disease-free equilibrium point with $R_0 < 1$. As it is taken as 0.0004, 0.0006, and 0.0008, Figure 2B demonstrates the global stability of the endemic equilibrium point with $R_0 > 1$. Figures 2C–F show the global stabilities of the equilibrium points with $n = 2$. Figures 3, 4 show the conclusions with $n = 3, 4$.

6 Conclusion and discussions

This paper constructs a general epidemic system with bilinear incidence rates. It contains n infected populations, where the first is the latent population. The transmission paths follow the top–down principle. We give all the disease transmission paths and find the number is equal to the sum of the combinatorial numbers. The basic reproduction number of our system has a reliable biological explanation and rigorous mathematical structure. It can be seen as the sum of the basic reproduction numbers of several infected populations with the ability to spread. We deform its structure and combine it with the disease transmission paths. A new method for calculating the basic reproduction number, the path analysis method, is proposed. The path analysis method is successfully applied to three representative examples containing different dimensions. Compared with the traditional next-generation method, the path analysis method greatly simplifies the calculation. It is possible to obtain the basic reproduction numbers of high-dimensional epidemic models without tedious calculations. The linear- and Volterra-type Lyapunov functions are used to prove the global stabilities of the disease-free and endemic equilibrium points. The global stability conditions are consistent with other studies. Simulations of the systems with 1, 2, 3, and 4 infected populations show that the infected populations converge to 0 when $R_0 < 1$ and to a constant when $R_0 > 1$. The path analysis method and the Volterra-type Lyapunov functions are not applicable to the systems with the nonlinear incidence rates, such as the Holling-type functions. For the simultaneous transmission of multiple infectious diseases, the path analysis method is also not feasible.

Data availability statement

The original contributions presented in the study are included in the article/Supplementary Material; further inquiries can be directed to the corresponding author.

Author contributions

YZ: conceptualization, methodology, software, and writing—original draft preparation. YD: visualization, investigation and supervision. MG: writing—reviewing and editing. All authors contributed to the article and approved the submitted version.

Funding

This work was supported by the National Natural Science Foundation of China (Grant No. 12271418).

Conflict of interest

The authors declare that the research was conducted in the absence of any commercial or financial relationships that could be construed as a potential conflict of interest.

Publisher's note

All claims expressed in this article are solely those of the authors and do not necessarily represent those of their affiliated organizations, or those of the publisher, the editors, and the reviewers. Any product that may be evaluated in this article, or claim that may be made by its manufacturer, is not guaranteed or endorsed by the publisher.

Supplementary material

The Supplementary Material for this article can be found online at: https://www.frontiersin.org/articles/10.3389/fphy.2023.1158814/full#supplementary-material

References

1. Kermack WO, McKendrick AG. Contributions to the mathematical theory of epidemics. II.—the problem of endemicity[J]. *Proc R Soc Lond Ser A, containing Pap a Math Phys character* (1932) 138(834):55–83.

2. Beretta E, Takeuchi Y. Global stability of an SIR epidemic model with time delays. *J Math Biol* (1995) 33(3):250–60. doi:10.1007/BF00169563

3. Korobeinikov A. Lyapunov functions and global stability for SIR and SIRS epidemiological models with non-linear transmission. *Bull Math Biol* (2006) 68: 615–26. doi:10.1007/s11538-005-9037-9

4. Wei W, Xu W, Song Y, Liu J. Bifurcation and basin stability of an SIR epidemic model with limited medical resources and switching noise. *Solitons & Fractals* (2021) 152:111423. doi:10.1016/j.chaos.2021.111423

5. Lei S, Jiang F, Su W, Chen C, Chen J, Mei W, et al. Clinical characteristics and outcomes of patients undergoing surgeries during the incubation period of COVID-19 infection. *EClinicalMedicine* (2020) 21:100331. doi:10.1016/j.eclinm.2020.100331

6. Chan-Yeung M, Xu RH. Sars: Epidemiology. *Respirology* (2003) 8:S9–S14. doi:10.1046/j.1440-1843.2003.00518.x

7. Eichner M, Dowell SF, Firese N. Incubation Period of Ebola hemorrhagic virus subtype zaire. *Osong Public Health Res Perspect* (2011) 2(1):3–7. doi:10.1016/j.phrp.2011.04.001

8. Schwartz IB, Smith HL. Infinite subharmonic bifurcation in an SEIR epidemic model. *J Math Biol* (1983) 18:233–53. doi:10.1007/bf00276090

9. Buonomo B, Lacitignola D. On the dynamics of an SEIR epidemic model with a convex incidence rate. *Ricerche di matematica* (2008) 57:261–81. doi:10.1007/s11587-008-0039-4

10. Wang X, Tao Y, Song X. Pulse vaccination on SEIR epidemic model with nonlinear incidence rate. *Appl Math Comput* (2009) 210(2):398–404. doi:10.1016/j.amc.2009.01.004

11. Efimov D, Ushirobira R. On an interval prediction of COVID-19 development based on a SEIR epidemic model. *Annu Rev Control* (2021) 51:477–87. doi:10.1016/j.arcontrol.2021.01.006

12. Wang L, Wang J, Zhao H, Shi YY, Wang K, Wu P, et al. Modelling and assessing the effects of medical resources on transmission of novel coronavirus (COVID-19) in Wuhan, China. *Math Biosci Eng* (2020) 17(4):2936–49. doi:10.3934/mbe.2020165

13. Nadim SS, Ghosh I, Chattopadhyay J. Short-term predictions and prevention strategies for COVID-19: A model-based study. *Appl Math Comput* (2021) 404:126251. doi:10.1016/j.amc.2021.126251

14. Das P, Nadim SS, Das S, et al. Dynamics of COVID-19 transmission with comorbidity: A data driven modelling based approach. *Nonlinear Dyn* (2021) 106:1197–211. doi:10.1007/s11071-021-06324-3

15. Péni T, Csutak B, Szederkényi G, Rost G. Nonlinear model predictive control with logic constraints for COVID-19 management. *Nonlinear Dyn* (2020) 102:1965–86. doi:10.1007/s11071-020-05980-1

16. Batabyal S, Batabyal A. Mathematical computations on epidemiology: A case study of the novel coronavirus (SARS-CoV-2). *Theor Biosciences* (2021) 140:123–38. doi:10.1007/s12064-021-00339-5

17. Biswas SK, Ghosh JK, Sarkar S, Ghosh U. COVID-19 pandemic in India: A mathematical model study. *Nonlinear Dyn* (2020) 102:537–53. doi:10.1007/s11071-020-05958-z

18. Ojo MM, Peter OJ, Goufo EFD, Panigoro HS, Oguntolu FA. Mathematical model for control of tuberculosis epidemiology. *J Appl Math Comput* (2023) 69(1):69–87. doi:10.1007/s12190-022-01734-x

19. Yin Q, Wang Z, Xia C, Bauch CT. Impact of co-evolution of negative vaccine-related information, vaccination behavior and epidemic spreading in multilayer networks. *Commun Nonlinear Sci Numer Simulation* (2022) 109:106312. doi:10.1016/j.cnsns.2022.106312

20. Ojo MM, Peter OJ, Goufo EFD, Nisar KS. A mathematical model for the co-dynamics of COVID-19 and tuberculosis. *Mathematics Comput Simulation* (2023) 207: 499–520. doi:10.1016/j.matcom.2023.01.014

21. Fan J, Yin Q, Xia C, et al. Epidemics on multilayer simplicial complexes[J]. *Proc R Soc A* (2022) 478(2261):20220059.

22. James Peter O, Ojo MM, Viriyapong R, Abiodun Oguntolu F. Mathematical model of measles transmission dynamics using real data from Nigeria. *J Difference Equations Appl* (2022) 28(6):753–70. doi:10.1080/10236198.2022.2079411

23. Wang Z, Xia C, Chen Z, Chen G. Epidemic propagation with positive and negative preventive information in multiplex networks. *IEEE Trans cybernetics* (2020) 51(3): 1454–62. doi:10.1109/TCYB.2019.2960605

24. D'Arienzo M, Coniglio A. Assessment of the SARS-CoV-2 basic reproduction number, R0, based on the early phase of COVID-19 outbreak in Italy. *Biosafety and health* (2020) 2(2):57–9. doi:10.1016/j.bsheal.2020.03.004

25. Amouch M, Karim N. Modeling the dynamic of COVID-19 with different types of transmissions. *J Chaos, Solitons Fractals* (2021) 150:111188. doi:10.1016/j.chaos.2021.111188

26. Ghosh JK, Biswas SK, Sarkar S, Ghosh U. Mathematical modelling of COVID-19: A case study of Italy. *Math Comput Simulation* (2022) 194:1–18. doi:10.1016/j.matcom.2021.11.008

27. Lv R, Li H, Sun Q, et al. Stability analysis and optimal control of a time-delayed panic-spreading model[J]. *Front Phys* (2022) 1026.

28. Zhang W, Ma X, Zhang Y, et al. Dynamical models of acute respiratory illness caused by human adenovirus on campus[J]. *Front Phys* (2022) 10:1325.

29. Wang L, Jin Z, Wang H. A switching model for the impact of toxins on the spread of infectious diseases. *J Math Biol* (2018) 77:1093–115. doi:10.1007/s00285-018-1245-7

30. Wei F, Xue R. Stability and extinction of SEIR epidemic models with generalized nonlinear incidence. *Math Comput Simulation* (2020) 170:1–15. doi:10.1016/j.matcom.2018.09.029

31. Pérez Á GC, Avila-Vales E, García-Almeida GE. Bifurcation analysis of an SIR model with logistic growth, nonlinear incidence, and saturated treatment. *Complexity* (2019) 2019:1–21. doi:10.1155/2019/9876013

32. Peter OJ, Panigoro HS, Ibrahim MA, et al. Analysis and dynamics of measles with control strategies: A mathematical modeling approach[J]. *Int J Dyn Control* (2023) 1–15.

33. Kammegne B, Oshinubi K, Babasola O, Peter OJ, Longe OB, Ogunrinde RB, et al. Mathematical modelling of the spatial distribution of a COVID-19 outbreak with vaccination using diffusion equation. *Pathogens* (2023) 12(1):88. doi:10.3390/pathogens12010088

34. Peter OJ, Yusuf A, Ojo MM, Kumar S, Kumari N, Oguntolu FA. A mathematical model analysis of meningitis with treatment and vaccination in fractional derivatives. *Int J Appl Comput Math* (2022) 8(3):117. doi:10.1007/s40819-022-01317-1

35. Ojo MM, Benson TO, Peter OJ, Goufo EFD. Nonlinear optimal control strategies for a mathematical model of COVID-19 and influenza co-infection. *Physica A: Stat Mech its Appl* (2022) 607:128173. doi:10.1016/j.physa.2022.128173

36. Melese AS, Makinde OD, Obsu LL. Mathematical modelling and analysis of coffee berry disease dynamics on a coffee farm. *Math Biosciences Eng* (2022) 19(7):7349–73. doi:10.3934/mbe.2022347

37. Ottaviano S, Sensi M, Sottile S. Global stability of SAIRS epidemic models. *Nonlinear Anal Real World Appl* (2022) 65:103501. doi:10.1016/j.nonrwa.2021.103501

38. Van den Driessche P, Watmough J. Reproduction numbers and sub-threshold endemic equilibria for compartmental models of disease transmission. *Math biosciences* (2002) 180(1-2):29–48. doi:10.1016/s0025-5564(02)00108-6

39. Meskaf A, Khyar O, Danane J, Allali K. Global stability analysis of a two-strain epidemic model with non-monotone incidence rates. *Solitons & Fractals* (2020) 133: 109647. doi:10.1016/j.chaos.2020.109647

40. Safi MA, Garba SM. Global stability analysis of SEIR model with holling type II incidence function[J]. *Comput Math Methods Med* (2012) 2012.

41. Li CL, Cheng CY, Li CH. Global dynamics of two-strain epidemic model with single-strain vaccination in complex networks. *Nonlinear Analysis: Real World Applications* (2023) 69:103738. doi:10.1016/j.nonrwa.2022.103738

42. Khan Z A, Alaoui A L, Zeb A, Tilioua M, Djilali S. Global dynamics of a SEI epidemic model with immigration and generalized nonlinear incidence functional. *Results in Physics* (2021) 27:104477. doi:10.1016/j.rinp.2021.104477

43. Saha S, Samanta G P, Nieto J J. Epidemic model of COVID-19 outbreak by inducing behavioural response in population. *Nonlinear dynamics* (2020) 102:455–87. Supplementary Material. doi:10.1007/s11071-020-05896-w